

See discussions, stats, and author profiles for this publication at: <https://www.researchgate.net/publication/231457836>

# Molecules in an electric field. Model for molecular geometry

ARTICLE *in* JOURNAL OF THE AMERICAN CHEMICAL SOCIETY · DECEMBER 1981

Impact Factor: 12.11 · DOI: 10.1021/ja00415a005

---

CITATIONS

27

---

READS

15

3 AUTHORS, INCLUDING:



Toshiaki Hayakawa

Advantest Laboratories Ltd., Sendai, Japan

3 PUBLICATIONS 61 CITATIONS

SEE PROFILE

# Molecules in an Electric Field. Model for Molecular Geometry<sup>1,2</sup>

Hiroshi Nakatsuji,\* Toshiaki Hayakawa, and Teijiro Yonezawa

Contribution from the Department of Hydrocarbon Chemistry, Faculty of Engineering, Kyoto University, Kyoto, Japan. Received February 18, 1981

**Abstract:** Electronic structures and geometries of molecules in an electric field are studied by the ab initio SCF MO method with floating AOs. The wave functions used satisfy the Hellmann-Feynman theorem. We have given an intuitive model which accounts for the change in geometry due to the electric field. The molecules studied here are CH<sub>4</sub>, C<sub>2</sub>H<sub>4</sub>, NH<sub>3</sub>, and CO in various orientations in the field.

## I. Introduction

The force concept based on the electrostatic theorem due to Hellmann and Feynman<sup>3</sup> gives a perspective viewpoint for electronic origins of the potential hypersurface in nuclear rearrangement processes.<sup>4</sup> A method to obtain numerically reliable Hellmann-Feynman forces through an improvement of wave function has recently been reported.<sup>5</sup>

In this series of studies,<sup>6,7</sup> we are developing a force and density concept, called ESF (electrostatic force) theory, for molecular geometry and chemical reaction. Here, we want to extend such studies to include geometries of molecules in external electric fields.<sup>8</sup>

An electric field applied to a molecule will cause a reorganization of the electron distribution, resulting in a change in the Hellmann-Feynman force acting on the constituent nuclei. The field also exerts a force directly on the nuclei. The resulting net force will induce a change in molecular geometry and vibrational force constants.<sup>8,9a</sup> Pancir and Zahradnik<sup>8</sup> studied geometries and vibrations of ethylene and acetylene in an electric field by the semiempirical INDO method. Here, we calculate a change in molecular geometry by ab initio molecular orbital calculations. The molecules studied here are CH<sub>4</sub>, C<sub>2</sub>H<sub>4</sub>, NH<sub>3</sub>, and CO in various orientations in the field. We study the origin of the force induced by the electric field, and give a model which helps us in predicting the geometries of molecules in external electric fields.

Now, there is very little knowledge on the geometry of molecules in the electric field.<sup>9a</sup> No experimental data seem to be available due to the difficulties in realizing strong electric fields. (We use in this study the field strength of 0.1 au ( $5 \times 10^{10}$  V/m).) However, such electric fields may appear in many phenomena if local fields are considered. For example, the electric field at 5.6 Å (10 au) apart from the positive ion of a single charge is 0.1 au. Further, in ordered systems such as nematic solvents, molecular crystals, and biopolymers, local electric fields seem to be able to become of this order. Though complex chemical interactions would be there in such systems,<sup>9b</sup> it is important to estimate the effects due solely to the electric field. There, one may need a guiding idea for the effects of the electric field on the electronic

structures, geometries, and vibrational frequencies of the molecules. The present study aims to give such a guiding idea.

In the next section we explain the methods of the present study. We have used ab initio floating wave functions which satisfy the Hellmann-Feynman theorem. The forces induced by the applied electric field are calculated and summarized in section III. The geometries optimized in the electric field are also given. In section IV, we analyze the ab initio results of section III using the concept of the Hellmann-Feynman force. This leads to an intuitive, simple model of molecular geometry in the electric field. It accounts for the changes in bond length and bond angle in agreements with the SCF MO results. The conclusion of the present study is given in the last section.

## II. Floating Wave Function

The electronic structure of molecules in a static electric field was calculated by an ab initio SCF MO method with a floating basis set.<sup>6d,10,11</sup> In the external electric field with strength  $E$ , the Fock matrix is given by

$$F_{rs} = H_{rs}^{\text{core}} - \mathbf{E} \cdot \mathbf{D}_{rs} + \sum_t \sum_u P_{tu} [(rs|tu) - \frac{1}{2}(rt|su)] \quad (1)$$

where  $\mathbf{D}_{rs}$  is the dipole moment matrix,  $\mathbf{D}_{rs} = \langle r|\mathbf{r}|s \rangle$ . The energy of the system is given by

$$E = \frac{1}{2} \sum_r \sum_s P_{rs} (H_{rs}^{\text{core}} - \mathbf{E} \cdot \mathbf{D}_{rs} + F_{rs}) + \sum_A \mathbf{E} Z_A + \sum_{A>B} \sum_Z Z_A Z_B / R_{AB} \quad (2)$$

where  $Z_A$  denotes nuclear charge. The force acting on a nucleus  $A$  is given by the Hellmann-Feynman theorem as

$$\mathbf{F}_A = Z_A \left\{ \int \rho(\mathbf{r}_1) \mathbf{r}_{A1} / r_{A1}^3 d\mathbf{r}_1 - \sum_{B(\neq A)} Z_B \mathbf{R}_{AB} / R_{AB}^3 + \mathbf{E} \right\} \quad (3)$$

where  $\rho(\mathbf{r}_1)$  is the electron density of the molecule. The present wave functions satisfy the Hellmann-Feynman theorem, since they are based on the floating AOs.<sup>10</sup> Namely, the centers of the AO bases are floated away from the nuclei and their positions are determined variationally.<sup>6d,11</sup> The effects of floating are summarized in Appendix A. Sadlej<sup>12</sup> has shown that the floating is effective for molecules in an electric field. When the nuclear framework is kept fixed, the effect of the external electric field on the force acting on nucleus  $A$  is written as

$$\begin{aligned} \Delta \mathbf{F}_A &= \mathbf{F}_A - \mathbf{F}_A^0 \\ &= Z_A \int \Delta \rho(\mathbf{r}_1) \mathbf{r}_{A1} / r_{A1}^3 d\mathbf{r}_1 + \mathbf{E} Z_A \\ &= \mathbf{F}_{\text{int}} + \mathbf{F}_{\text{ext}} \end{aligned} \quad (4)$$

$$\Delta \rho(\mathbf{r}_1) = \rho(\mathbf{r}_1) - \rho^0(\mathbf{r}_1) \quad (5)$$

$$\int \Delta \rho(\mathbf{r}_1) d\mathbf{r}_1 = 0 \quad (6)$$

(10) A. C. Hurley, *Proc. R. Soc. London, Ser. A*, **226**, 170, 179, 193 (1954); A. C. Hurley in "Molecular Orbitals in Chemistry, Physics and Biology", P.-O. Löwdin and B. Pullman, Eds., Academic Press, New York, N.Y., 1964, p 161.

(11) H. Nakatsuji, K. Matsuda, and T. Yonezawa, *Chem. Phys. Lett.*, **54**, 347 (1978).

(12) A. J. Sadlej, *Mol. Phys.*, **34**, 731 (1977).

(1) Part 8 of the series entitled Electrostatic Force Theory for a Molecule and Interacting Molecules.

(2) Part of this study was presented at the third International Congress of Quantum Chemistry, Kyoto, November 1979.

(3) H. Hellmann, "Einführung in die Quantenchemie", Deuticke, Vienna, 1937, p 285; R. P. Feynman, *Phys. Rev.*, **56**, 340 (1939).

(4) B. M. Deb, Ed., "The Force Concept in Chemistry", Van Nostrand Reinhold, New York, N.Y., 1981.

(5) H. Nakatsuji, K. Kanda, and T. Yonezawa, *Chem. Phys. Lett.*, **75**, 340 (1980); H. Nakatsuji, T. Hayakawa, and M. Hada, *ibid.*, **80**, 94 (1981).

(6) (a) Parts 1-3: H. Nakatsuji, *J. Am. Chem. Soc.*, **95**, 345, 354, 2084 (1973). (b) Part 4: H. Nakatsuji and T. Koga, *ibid.*, **96**, 6000 (1974). (c) Parts 5 and 6: H. Nakatsuji, *ibid.*, **96**, 24, 30 (1974). (d) Part 7: H. Nakatsuji, S. Kanayama, S. Harada, and T. Yonezawa, *ibid.*, **100**, 7528 (1978).

(7) H. Nakatsuji and T. Koga, ref 4, Chapter 3.

(8) J. Pancir and R. Zahradnik, *Helv. Chim. Acta*, **61**, 59 (1978). J. Pancir and I. Haslingerova, *Collect. Czech. Chem. Commun.*, **45**, 2474 (1980).

(9) (a) Extensive references for the studies of the effects of an electric field are found in ref 8. (b) H. Nakatsuji, I. Morishima, H. Kato, and T. Yonezawa, *Bull. Chem. Soc. Jpn.*, **44**, 2010 (1971).

**Table I.** Stability of Molecules in Various Orientations in an Electric Field

molecule	electric field, <sup>a</sup> au	energy, <sup>b</sup> au	
		at nonfield optimal geometry	at optimal geometry under electric field
CH <sub>4</sub>	$E = 0.0$	-39.72630	
type I	$E_z = 0.1$	-39.75554	-39.75779
type I	$E_z = -0.1$	-39.75376	-39.75436
type II	$E_z = 0.1$	-39.75462	-39.75700
C <sub>2</sub> H <sub>4</sub>	$E = 0.0$	-77.09226	
	$E_x = 0.1$	-77.16692	-77.17410
	$E_z = 0.1$	-77.12698	-77.13021
NH <sub>3</sub>	$E = 0.0$	-55.44614	
	$E_z = 0.0$	-55.53230	-55.53463
	$E_z = -0.1$	-55.37784	
CO	$E = 0.0$	-111.22547	
	$E_x = 0.1$	-111.25257	-111.25498
	$E_x = -0.1$	-111.26388	-111.26404

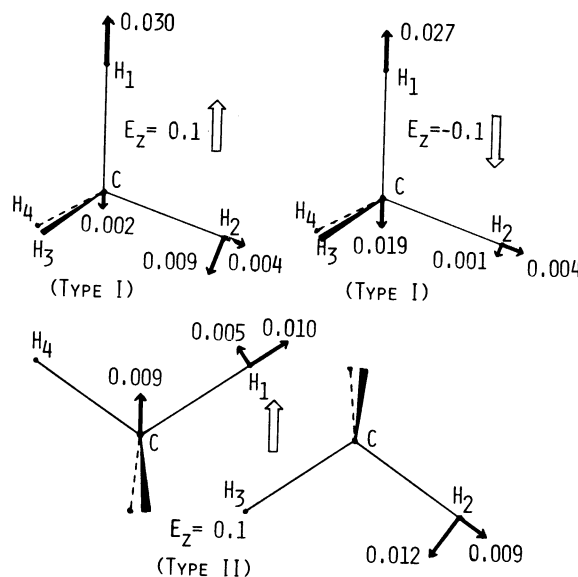
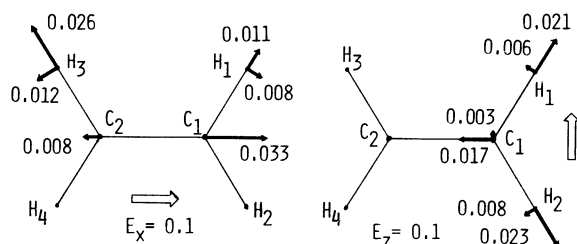
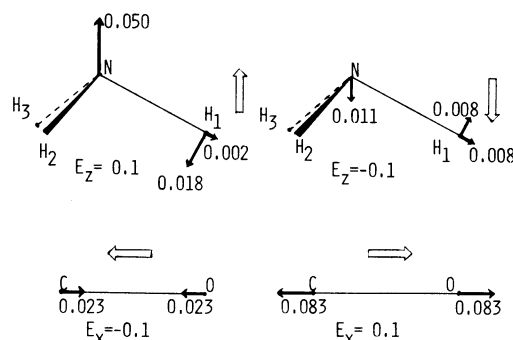
<sup>a</sup> Direction of the applied electric field is defined in Figures 1–3.<sup>b</sup> The energy obtained by the nonfloating AOs is given in both stages of calculation.

where  $F_A^0$  and  $\rho^0(r_i)$  denote the force and density at zero external field.  $\Delta\rho(r_i)$  shows the reorganization of electron density due to the electric field. When the calculation is carried out at the geometry which is equilibrium in the absence of the external field (which is referred to as *nonfield-equilibrium geometry*),  $F_A^0$  is zero and  $\Delta F_A = F_A$ . Equation 4 shows that the force induced by the electric field,  $\Delta F_A$ , is the sum of the force due to the change in the electron density,  $\Delta\rho$ , and the force due to the electrostatic interaction of the nuclear charge with the external field. We denote hereafter the first and second terms as internal force  $F_{int}$  and external force  $F_{ext}$ , respectively.

The molecules studied here are CH<sub>4</sub>, C<sub>2</sub>H<sub>4</sub>, NH<sub>3</sub>, and CO. The electric field was applied in various directions with the strength of 0.1 au ( $\sim 5.1 \times 10^{10}$  V/m). (The direction of the electric field is from negative pole to positive one.) The calculation was carried out using STO-3G bases with standard scale factors.<sup>13</sup> For NH<sub>3</sub>, we have used GTO expansion given by Stewart.<sup>14</sup> The nonfield-equilibrium geometries are CH = 1.083 Å for CH<sub>4</sub>,<sup>15</sup> CH = 1.090 Å, CC = 1.389 Å, and  $\angle HCH = 113.0^\circ$  for C<sub>2</sub>H<sub>4</sub>,<sup>15</sup> NH = 1.033 Å and  $\angle HNH = 100.8^\circ$  for NH<sub>3</sub>,<sup>6d</sup> and CO = 1.146 Å for CO.<sup>15</sup> Floating wave functions were calculated for these molecules at the nonfield-equilibrium geometries. We have floated all of the AOs simultaneously and determined optimal centers by making all the AO errors (AO forces) vanish identically.<sup>6d</sup> The geometry optimization under the electric field was carried out by the energy gradient method without floating.<sup>16</sup>

### III. Molecular Geometry in an Electric Field

In this section we show the geometry of molecules in the electric field calculated by the ab initio SCF MO method. Table I shows the energy of the molecules with and without external electric field. It shows a preferred orientation of the molecules in the electric field. (The orientations of the molecules in the field are defined in Figures 1–3.) For methane, the orientation type I with  $E_z = +0.1$  au is calculated to be most preferable, though the energy differences among various orientations are small. Ethylene prefers its double bond to be parallel with the field, as expected from its polarizability tensor. Pancir and Zahradnik<sup>8</sup> suggested that the orientation  $E_z = 0.1$  au is rotationally unstable (i.e., potential maximum). Polar molecules NH<sub>3</sub> and CO orient themselves in

**Figure 1.** Force in an electric field for CH<sub>4</sub>. The stability of the orientation is  $E_z = 0.1$  (type I),  $E_z = 0.1$  (type II),  $E_z = -0.1$  (type I) in decreasing order. Values are given in atomic units.**Figure 2.** Force in an electric field for C<sub>2</sub>H<sub>4</sub>. The left orientation is more stable than the right one. Values are given in atomic units.**Figure 3.** Force in an electric field for NH<sub>3</sub> and CO. The left orientation is more stable than the right one. Values are given in atomic units.

the direction as expected from their permanent dipole moments. Interesting behavior of NH<sub>3</sub> when it is in the field with  $E_z = -0.1$  au will be mentioned below.

When an electric field is applied to a molecule, the electron density will be reorganized and the forces will be induced on the constituent nuclei. Figures 1–3 show such forces calculated from the floating wave functions which satisfy the Hellmann–Feynman theorem. They are connected to the electron density of the system by eq 3 and 4. Since the geometry is at the nonfield-equilibrium geometry,  $F_A^0$  in eq 4 vanishes identically so that the forces  $F_A$  shown in Figures 1–3 are equal to  $\Delta F_A$ . The nuclei will move along these forces and reach the geometry optimal under the electric field. In Tables II–IV, we have given such geometries optimized by the SCF MO calculations.

Figure 1 shows that under the electric field, the C–H length of methane will become longer irrespective of the orientation of the molecule. This is confirmed in Table II. The extent of elongation is parallel to the cosine between the field and the bond;

(13) W. J. Hehre, R. F. Stewart, and J. A. Pople, *J. Chem. Phys.*, **51**, 2657 (1969).(14) R. F. Stewart, *J. Chem. Phys.*, **52**, 431 (1970).(15) W. A. Lathan, L. A. Curtiss, W. J. Hehre, J. B. Listle, and J. A. Pople, *Prog. Phys. Org. Chem.*, **11**, 175 (1974).(16) J. Gerratt and I. Mills, *J. Chem. Phys.*, **49**, 1719 (1968); P. Pulay, *Mol. Phys.*, **17**, 197 (1969); A. Komornicki, K. Ishida, K. Morokuma, R. Ditchfield, and M. Conrad, *Chem. Phys. Lett.*, **45**, 595 (1977).

Table II. Optimal Geometry of CH<sub>4</sub> in an Electric Field

orientation <sup>a</sup>	electric field, au	<i>r</i> (C-H <sub>1</sub> ), Å	<i>r</i> (C-H <sub>2</sub> ), Å	∠H <sub>1</sub> CH <sub>2</sub> , deg	∠H <sub>1</sub> CH <sub>4</sub> , deg	∠H <sub>2</sub> CH <sub>3</sub> , deg
type I	<i>E</i> = 0.0	1.0830	1.0830	109.47	109.47	109.47
	<i>E<sub>z</sub></i> = 0.1	1.1175 (+0.0345) <sup>b</sup>	1.0864 (+0.0034)	113.04 (+3.57)	113.04 (+3.57)	105.68 (-3.79)
type I	<i>E<sub>z</sub></i> = -0.1	1.1091 (+0.0261)	1.0873 (+0.0043)	109.70 (+0.23)	109.70 (+0.23)	109.24 (-0.23)
	<i>E<sub>z</sub></i> = 0.1	1.0946 (+0.0116)	1.0933 (+0.0103)	111.31 (+1.84)	107.28 (-2.19)	104.40 (-5.07)

<sup>a</sup> For orientation and numbering of atoms, see Figure 1. <sup>b</sup> Values in parentheses show the change due to the electric field.Table III. Optimal Geometry of C<sub>2</sub>H<sub>4</sub> in an Electric Field<sup>a</sup>

electric field, au	<i>r</i> (C <sub>1</sub> -H <sub>1</sub> ), Å	<i>r</i> (C <sub>1</sub> -H <sub>2</sub> ), Å	<i>r</i> (C <sub>2</sub> -H <sub>3</sub> ), Å	<i>r</i> (C <sub>1</sub> -C <sub>2</sub> ), Å	∠H <sub>1</sub> C <sub>1</sub> H <sub>2</sub> , deg	∠H <sub>3</sub> C <sub>2</sub> H <sub>4</sub> , deg	∠H <sub>1</sub> C <sub>1</sub> C <sub>2</sub> , deg
<i>E</i> = 0.0	1.0790	1.0790	1.0790	1.3050	115.40	115.40	122.30
<i>E<sub>x</sub></i> = 0.1	1.0927 (+0.0137) <sup>b</sup>	1.0927 (+0.0137)	1.1128 (+0.0338)	1.3454 (+0.0404)	110.34 (-5.06)	107.24 (-8.16)	124.83 (+2.53)
<i>E<sub>z</sub></i> = 0.1	1.1053 (+0.0263)	1.1034 (+0.0244)	1.1053 (+0.0263)	1.3096 (+0.0046)	119.66 (+4.26)	119.66 (+4.26)	120.02 (-2.28)

<sup>a</sup> For orientation and numbering of atoms, see Figure 2. <sup>b</sup> Values in parentheses show the change due to the electric field.Table IV. Optimal Geometry of NH<sub>3</sub> and CO in an Electric Field<sup>a</sup>

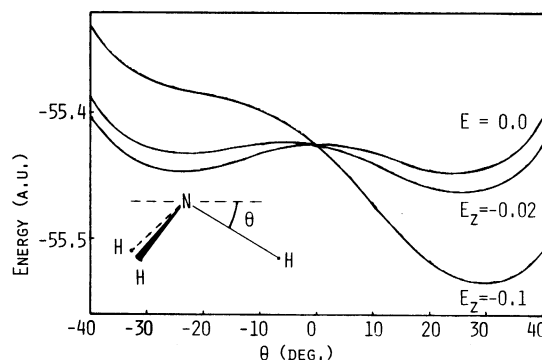
molecule	electric field, au	<i>r</i> (N-H) or <i>r</i> (C-O), Å	∠HNH, deg
NH <sub>3</sub>	<i>E</i> = 0.0	1.0330	100.75
	<i>E<sub>z</sub></i> = 0.1	1.0389 (+0.0059) <sup>b</sup>	96.29 (-4.46)
CO	<i>E</i> = 0.0	1.1456	
	<i>E<sub>x</sub></i> = 0.1	1.1780 (+0.0324)	
	<i>E<sub>x</sub></i> = -0.1	1.1380 (-0.0076)	

<sup>a</sup> For orientation see Figure 3. <sup>b</sup> Values in parentheses show the change due to the electric field.

the largest is the C-H<sub>1</sub> bond in type I, which is parallel to the field, next is the C-H bond in type II, and the smallest is the C-H<sub>2</sub> bond in type I. From Figure 1, the H<sub>1</sub>CH<sub>2</sub> angle in type I orientation is expected to increase for both *E<sub>z</sub>* = ±0.1 au. The H<sub>1</sub>CH<sub>4</sub> and H<sub>2</sub>CH<sub>3</sub> angles in type II orientation will decrease. This is confirmed in Table II. Further, the existence of optimal geometry shows that methane is stable to dissociation at least up to *E* = 0.1 au.

Figure 2 is for ethylene. Again, all of the bonds are expected to be elongated. Though the force acting on the C<sub>1</sub> nucleus at *E<sub>z</sub>* = 0.1 au apparently seems to shorten the C-C length, the force acting on the CH<sub>2</sub> groups works to elongate the C-C distance. This is confirmed in Table III. When the C-C bond is parallel to the field (stable orientation), it is elongated as much as 0.0404 Å. For the bond angles, Figure 2 and Table III show that when *E<sub>x</sub>* = 0.1 au both H<sub>1</sub>C<sub>1</sub>H<sub>2</sub> and H<sub>3</sub>C<sub>2</sub>H<sub>4</sub> angles decrease by the amounts of 5.1° and 8.2°, respectively, and when *E<sub>z</sub>* = 0.1 au, the HCH angle will increase by 4.3°. Further, up to the field strength of *E* = 0.1 au, ethylene will be stable to dissociation.

The upper part of Figure 3 is for ammonia. Again the bond will become longer in both directions of the field. In a stable orientation (left-hand side) the HNH angle will become smaller. Table IV confirms these trends. When the field is reversed (*E<sub>z</sub>* = -0.1 au), ammonia will show an interesting behavior. As seen in the right-hand side of Figure 3, the HNH angle will increase. In Figure 4, we have shown the potential energy curve along the inversion mode of NH<sub>3</sub>. We found that when *E<sub>z</sub>* = -0.1 au, the barrier disappears. When *E<sub>z</sub>* = 0.0 au, the barrier height was calculated to be 13.2 kcal/mol (the experimental value is 5.8 kcal/mol).<sup>17</sup> When *E<sub>z</sub>* = -0.02 au, it decreases to 4.6 kcal/mol. This means that in the electric field stronger than *E<sub>z</sub>* ~ -0.03 au, ammonia can take stable orientations not through rotation

Figure 4. Potential energy curve along the inversion mode for NH<sub>3</sub> in an electric field with strength *E<sub>z</sub>* = 0.0, -0.02, and -0.1 au.

but through inversion. This is interesting when the molecule is crowded in space as in biological systems.

The lower side of Figure 3 shows the results for carbon monoxide. For CO the stable orientation is *E<sub>x</sub>* = -0.1 au as shown in Table I. This is due to the atomic dipole on carbon. This orientation is the reverse of that expected from the electronegativities of the atoms. Figure 3 shows that the CO length will become shorter in this orientation. This is the first, interesting example of bond-length shortening in the electric field. The reason for this will be discussed below. In the orientation *E<sub>x</sub>* = 0.1 au, the CO length will become longer. These predictions are confirmed in Table IV which shows the optimal geometry in the field.

#### IV. Model for Molecular Geometry in an Electric Field

Here we want to obtain a predictive model for geometries of molecules in electric fields. Since the forces shown in Figures 1-3 are connected, by eq 4, with the change in the electron density  $\Delta\rho(\mathbf{r}_1)$  induced by the applied field, one may get an insight from the contour map of  $\Delta\rho(\mathbf{r}_1)$ .

First we study ethylene in the field *E<sub>x</sub>* = 0.1 au (stable orientation). In Figure 5 we have given the  $\Delta\rho$  map, the intersection being on the *xz* plane (molecular plane) for the upper part and on the *xy* plane ( $\pi$  plane) for the lower part. Solid and broken lines show respectively an increase and decrease in electron density.  $\Delta\rho$  is almost antisymmetric with respect to the *yz* plane which bisects the midpoint of the C-C bond. This property is readily deduced from the perturbation theoretic viewpoint as given in Appendix B. Group theoretic considerations of molecules in an electric field<sup>18</sup> should also be useful. On the molecular plane (upper figure) electrons flow from H<sub>3</sub> and H<sub>4</sub> to C<sub>2</sub> and from C<sub>1</sub> to H<sub>1</sub> and H<sub>2</sub>. Near the midpoint of the C-C bond, the  $\sigma$  bond

(17) J. D. Swalen and J. A. Ibers, *J. Chem. Phys.*, **36**, 1914 (1962).(18) J. K. G. Watson, *Can. J. Phys.*, **53**, 2210 (1975).

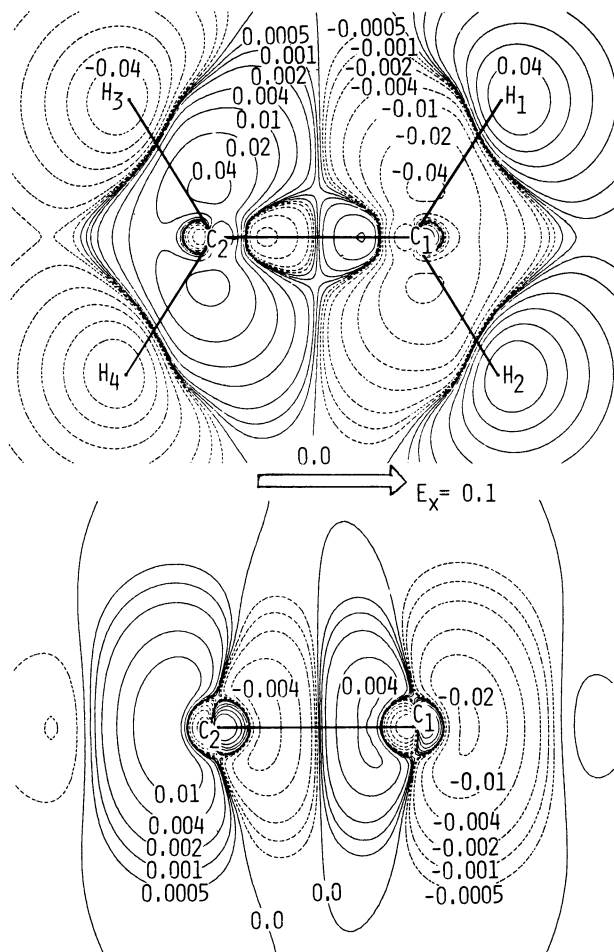


**Figure 5.** Reorganization of electron density of  $C_2H_4$  in the electric field,  $E_x = +0.1$  au. The plane of intersection includes the C-C bond and is parallel (upper figure) and perpendicular (lower one) to the molecular plane. Solid and broken lines show respectively an increase and decrease in electron density.

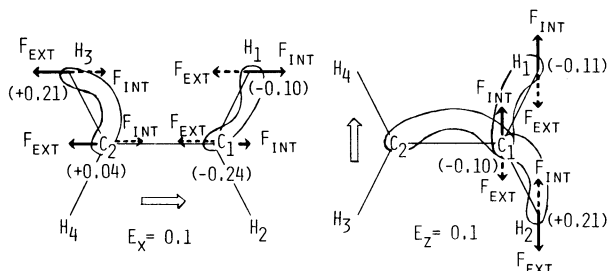


**Figure 6.** Picture of the bent bond of ethylene in the electric field and the direction of  $F_{int}$  and  $F_{ext}$  acting on the terminal nuclei. The direction of the predicted force is given by the solid arrow. Values in parentheses show the reorganized gross atomic charge obtained in the electric field. The left orientation is more stable than the right one.

density flows in the direction of the field. On the  $\pi$  plane (lower figure) the  $\pi$  electron flows from  $C_2$  to  $C_1$ . In total electrons flow from the methylene in the left-hand side to the methylene in the right-hand side. We have shown in Figure 6 the gross atomic charge<sup>19</sup> in the field. When  $E_z = 0.0$  au, the gross atomic charge is  $+0.051$  for H and  $-0.102$  for C. Looking at the density along the C-H bond (Figure 5), we notice that the bond density is bent in the direction of the electric field. We may illustrate such a bent bond as shown in the left-hand side of Figure 6. The electrons in such a bent bond will attract the terminal proton in the direction of the field. This is a main source of  $F_{int}$  acting on the terminal protons.<sup>20</sup> They are also attracted by the external

**Table V.** Gross Atomic Charge at Zero External Field

molecule	atom	gross charge
$CH_4$	C	$-0.188$
	H	$+0.047$
$C_2H_4$	C	$-0.102$
	H	$+0.051$
$NH_3$	N	$-0.408$
	H	$+0.136$
CO	C	$+0.155$
	O	$-0.155$

field ( $F_{ext}$  in eq 4) in the reverse direction of the field. The net force is a result of a balance of  $F_{int}$  and  $F_{ext}$ . The same is true for carbon. Since electrons flow in the direction of the field,  $F_{int}$  on C is in the direction of the field and  $F_{ext}$  is in the reverse direction of the field.<sup>21</sup> Analysis of  $F_{int}$  by means of the changes in the atomic dipole (AD), exchange (EC), and extended gross charge (EGC) forces<sup>6a,11</sup> has supported the above picture.<sup>20,21</sup>

We now postulate that when the number of electrons near the nucleus is more than the nuclear charge, the effect of the electron cloud,  $F_{int}$ , would overcome the effect of the field on the bare nucleus, i.e.,  $F_{ext}$ , and vice versa. As a measure of electron population near the nucleus A, we may use the Mulliken's gross atomic charge,<sup>19</sup>  $\delta_A$ , for the molecule in the electric field. Namely we postulate that

$$\text{if } \delta_A < 0, |F_A^{int}| > |F_A^{ext}| \quad \text{if } \delta_A > 0, |F_A^{int}| < |F_A^{ext}| \quad (7)$$

In the former case,  $F_A$  is in the direction of the electric field, and in the latter case,  $F_A$  is in the reverse direction of the field. The above model is based on the local nature of the force operator,  $r_{AI}/r_{AI}^3$ , which decreases rapidly as  $r_{AI}$  increases. This picture is consistent with the picture based on the interaction of the charged particles in the electric field, the molecule being considered as a linked charged particle and the charge being estimated by the gross atomic charge. Note that gross atomic charge is a quantity which is calculated or estimated much more easily than the force itself.

In Figure 6 the gross atomic charge of ethylene in the field is shown. The gross atomic charge in the absence of the field is shown in Table V. From the above model we predict that in the field of  $E_x = +0.1$  au (left-hand side), the  $H_1$  and  $C_1$  nuclei will receive the force in the direction of the field since their gross atomic charges are negative, and the reverse force will act on  $H_3$  and  $C_2$  nuclei since their gross atomic charges are positive. This prediction agrees with the ab initio result shown in Figure 2. As a result, all bonds will become longer and angles  $\angle H_1C_1H_2$  and  $\angle H_3C_2H_4$  will decrease in the field as confirmed in Table III.

Next, we consider ethylene in the field  $E_z = 0.1$  au. Due to Pancir and Zahradnik,<sup>8</sup> this orientation is at potential maximum and so is rotationally unstable. Figure 7 shows the map of  $\Delta\rho$  induced by the field. The intersection is on the  $xz$  plane (molecular  $\sigma$  plane) for the upper part and on the  $xy$  plane ( $\pi$  plane) for the lower part. Again the  $\Delta\rho$  map is almost antisymmetric with respect to the  $\pi$  plane (Appendix B). The density decreases near  $H_2$ , increases near  $H_1$ , and is strongly polarized near the carbon atom. Along the C-C and C-H bonds, the bond density is bent in the direction of the field as illustrated in Figure 6.<sup>20</sup> Along the  $C_1$ - $C_2$  axis, the density does not change. It is interesting to note that in the  $\pi$  plane the density near the carbon moves inside of the C-C bond. (See the enlarged figure in lower side of Figure

(20) Partitioning of the transverse element of the force  $F_{int}^H$  into atomic dipole (AD), exchange (EC), and extended gross charge (EGC) forces<sup>6,7</sup> has shown that the effect of the electric field on this force is mainly due to the change in the AD and EC(H-C) forces. This confirms that the bent bond as depicted in Figure 6 is certainly the origin of this force.<sup>6a,11</sup>

(21) Along the bond, the flow of gross electron density in the direction of the field seems to be important. This was shown from the analysis of  $F_{int}$  into the change in the AD, EC, and EGC forces.<sup>6a,11</sup> Namely, the main source of  $F_{int}$  along the bond was shown to be due to the change in the EGC force induced by the electric field.

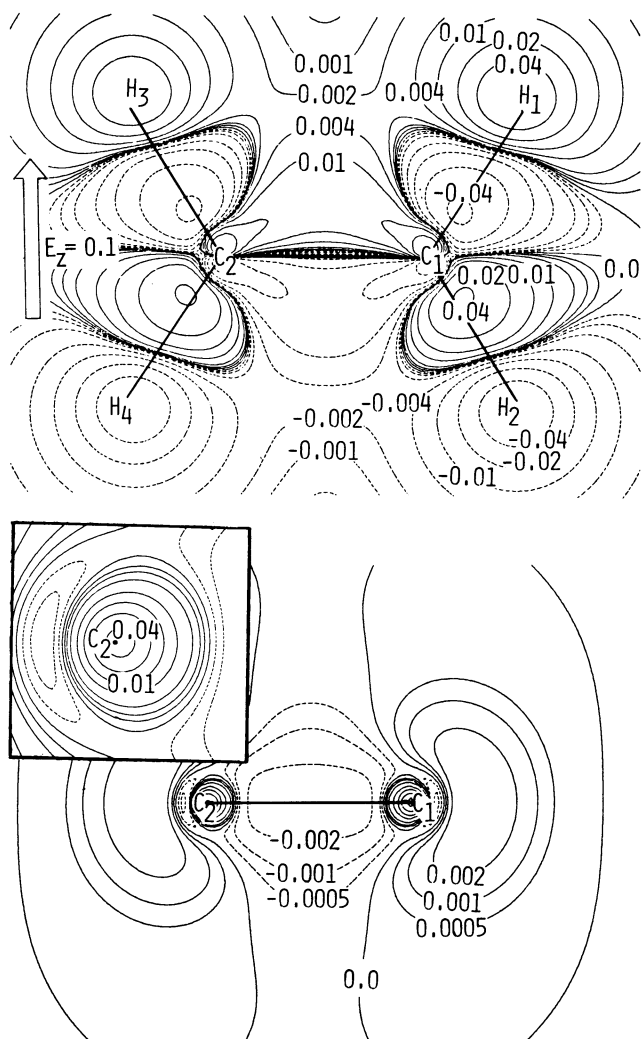


**Figure 7.** Reorganized electron density of  $C_2H_4$  in an electric field,  $E_z = 0.1$  au. The plane of intersection includes the C-C bond and is parallel (upper figure) and perpendicular (lower one) to the molecular plane. Solid and broken lines show an increase and decrease, respectively. In the lower figure, the density increased just inside of the carbon  $C_2$  is enlarged. There the contour values are an order of magnitude larger than those outside of the carbons.

7.) The increase outside of the bond is small.

Referring to the gross atomic charge shown in Figure 6 (right-hand side), we expect from eq 7 that the force along the  $z$  axis is in the  $+z$  direction for the nuclei  $H_1$  and  $C_1$  and the  $-z$  direction for the  $H_2$  proton. The HCH angle will therefore increase in the field. This is in accord with the result of the ab initio calculation shown in Figure 2. The force in the  $-x$  direction acting on  $C_1$  (Figure 2) is not described by the above model, because it is perpendicular to the field. This force is understood as an attraction of  $C_1$  by the electron density moved inside of the C-C bond in the  $\pi$  plane (see lower part of Figure 7).

In Figure 8 the gross atomic charge in the field and the direction of the force predicted from the above model are shown for  $CH_4$ ,  $NH_3$ , and CO. Comparing with Figures 1 and 3 we see that the predicted directions of the forces agree mostly with those calculated by the ab initio SCF method. The exceptions are the force acting on the carbon of methane in the field  $E_z = 0.1$  au (type I), and the force in CO in its stable orientation  $E_x = -0.1$  au. For CO, however, we notice that in the field  $E_x = -0.1$  au the gross charges of C and O have changed even their signs from the field-free values shown in Table V. This means that in weaker fields in the  $-x$  direction, the gross charge in the field is  $\delta+$  for carbon and  $\delta-$  for oxygen so that the above model predicts the forces which work to shorten the CO length in agreement with the result shown in Figure 3.

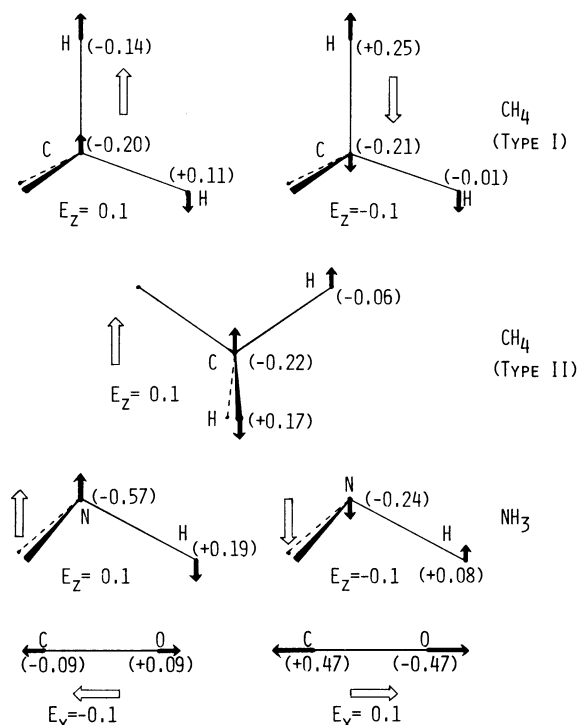
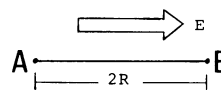


**Figure 8.** Gross atomic charge in the electric field and the direction of the force predicted from the model, eq 7. Among the orientations the left one is most stable and the right one most unstable.

Thus, the above model accounts for most of the ab initio results obtained in this paper. The change in bond angle is accounted for without exceptions. The bond is expected to become longer for all the homopolar bonds and for most heteropolar bonds in the field applied from electropositive atom to electronegative atom (stable orientation for most molecules). Vibrational force constants are also expected to become smaller in these cases. In different orientations, the heteropolar bonds can become shorter for some range of field strengths.

**Different View for Bond Length Change.** The above model has thus given predictions which are in general agreement with the SCF method for both bond angles and bond lengths. For bond lengths, however, there is another model which gives almost the same predictions as the above one, but complements the oversimplification of the above model.

Let us consider a homopolar diatomic molecule AB in the electric field with the strength  $E$ . The field is applied parallel with the bond from A to B as



We consider the electronic structure by a simple Hückel method assigning one AO for each atom. Referring to eq 1 the Fock matrix is written as

$$F = \begin{vmatrix} \alpha & \beta \\ \beta & \alpha \end{vmatrix} - E \begin{vmatrix} -R & 0 \\ 0 & R \end{vmatrix} \quad (8)$$

where the first matrix on the right-hand side is the field-free matrix and the second one the dipole moment matrix, the origin being the midpoint of AB and  $2R$  being the bond length. Using the zero-differential overlap approximation we have calculated bond and atomic densities as a function of  $E$  and shown the results in Figure 9.

In the bonding configuration  $(\phi)^1(\phi^*)^0$ , the atomic density decreases on A and increases on B as  $E$  increases; i.e., electronic charge flows from A to B in the direction of the field. The bond density decreases monotonously flowing again to atom B. The maximum is at the field-free position. In the antibonding configuration  $(\psi)^0(\psi^*)^1$ , however, the density flows in reverse and

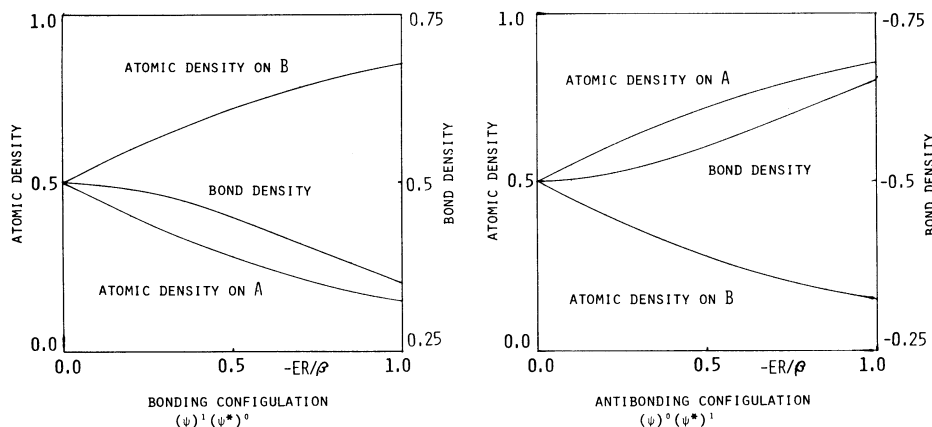


**Figure 9.** Atomic and bond densities for bonding and antibonding configurations of the homopolar diatomic molecule AB in the electric field with strength  $E$ . Bond length is  $2R$  and the field is parallel to the bond from A to B.

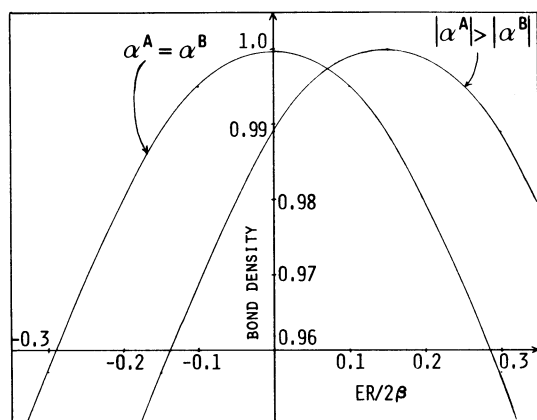


**Figure 10.** Bond density vs. electric field strength for the heteropolar diatomic molecule AB by the Hückel model.

the bond density increases as the field is applied. For a stable molecule, the bonding interaction should be larger than the antibonding interaction. We therefore expect that the bond will become longer and the force constant will become smaller in the electric field. This is the trend which actually was observed by the ab initio SCF calculations.

When the molecule is heteropolar, different behavior may occur. The Fock matrix may be written as

$$F = \begin{vmatrix} \alpha_A & \beta & -E \\ \beta & \alpha_B & 0 \\ -E & 0 & R_B \end{vmatrix} \quad (9)$$

where  $R_A + R_B = 2R$ . The origin was so chosen as the moment matrix is given by the second term of eq 9. In Figure 10, the bond density for the bonding configuration is plotted against the field strength. When  $\alpha_A = \alpha_B$  (homopolar), the bond density is maximum at  $E = 0.0$  au, but when  $\alpha_A \neq \alpha_B$  (heteropolar) the maximum moves away from  $E = 0.0$  au. When atom A is more electronegative than atom B ( $|\alpha_A| > |\alpha_B|$ ), atom A has excess electrons (negatively charged) at  $E = 0.0$  au. When the field is applied in the direction from A to B, the excess charge on A flows not only to B but also to the bonding region so that the bond density increases as shown in Figure 10. If this effect is significant, the bond length can become shorter as the electric field is applied. Figure 10 shows further that such change is limited only in some range of the field strength. Moreover, in most cases, this orientation is unfavorable because the dipole moments of most molecules are determined by the charge dipole. Carbon monoxide is a very special exception to this since its dipole moment is chiefly determined by the atomic dipole on carbon. Thus, we may expect for most molecules that in stable orientations, the bond will become longer in an electric field.

In order to test the above idea, we have applied the electric field to carbon monoxide from O to C in the ab initio SCF MO cal-

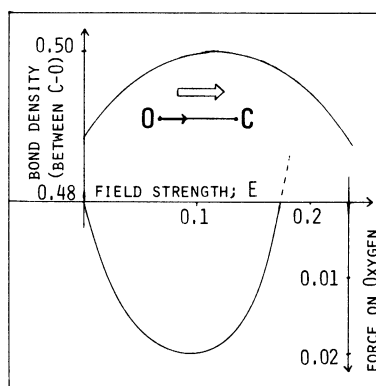


**Figure 11.** Bond density and force vs. electric field strength for the CO calculated by the ab initio SCF MO method (nonfloating).

culations. Figure 11 shows the force acting on oxygen and the bond density vs. the field strength. Up to the strength of 0.18 au, the bond is shown to become shorter in agreement with the above model. The bond density increases in this range of field strengths. If the field is in the reverse direction or it is stronger than 0.18 au, the bond will become longer.

Pancir and Haslingerova<sup>8</sup> found by the INDO calculations of acetylene that in an electric field all the bond lengths become longer and their bond strengths decrease. This result accords with the above model.

## V. Conclusion

In this paper we have studied the geometry of molecules in an electric field. In the first stage, the force induced by the electric field at the nonfield-equilibrium geometry is calculated using ab initio floating wave functions. These forces are connected to the electron density of the system by the Hellmann-Feynman theorem. Further, we have determined optimal geometries in the electric field by the ab initio SCF MO method. In the second stage, we have searched for a simple model which accounts for the change in geometry induced by the electric field. The simplicity of the Hellmann-Feynman force as expressed by eq 3 and 4 is used for the analysis. As a result, we have given a model as expressed by eq 7. This model accounts for most of the ab initio results obtained in this study. The change in bond angle is accounted for without exceptions. The bond is expected to become longer for all the homopolar bonds and for the heteropolar bonds in the field applied from electropositive atom to electronegative atom (stable orientation for most molecules). In these cases, the vibrational force constants are expected to become smaller. In different orientations, the heteropolar bonds can become shorter in some range of the field strength. For the change in bond length we have shown another model based on a simple Hückel consideration. It complements the above model and gives almost the same predictions. The present model thus is a guide for predicting the geometry of molecules in electric fields. It would become useful when strong

Table VI. Energy Lowering due to the Floating of the AOs

molecule	electric field, <sup>a</sup> au	$\Delta E$ , <sup>b</sup> $\times 10^2$ au
CH <sub>4</sub>	$E = 0.0$	-0.376
	$E_z = 0.1$ (type I)	-1.286
	$E_z = -0.1$ (type I)	-1.616
C <sub>2</sub> H <sub>4</sub>	$E_z = 0.1$ (type II)	-1.621
	$E = 0.1$	-1.833
	$E_x = 0.1$	-2.476
NH <sub>3</sub>	$E_z = 0.1$	-2.614
	$E = 0.0$	-2.209
	$E_z = 0.1$	-1.404
CO	$E_z = -0.1$	-4.597
	$E = 0.0$	-6.211
	$E_x = 0.1$	-6.108
	$E_x = -0.1$	-6.700

<sup>a</sup> Orientation of the molecule in the electric field is defined in Figures 1-3. <sup>b</sup> Energy difference is defined by  $\Delta E = E(\text{float}) - E(\text{nonfloat})$ .

Table VII. Optimal Floating Distance of the AOs from the Nucleus for Ethylene

electric field, au	nucleus	AO	floating distance, <sup>a</sup> Å	
			X direction	Z direction
$E = 0.0$	C <sub>1</sub>	1s	0.0000325	0.0
		2s	0.0219	0.0
		2p <sub>x</sub>	-0.0085	0.0
		2p <sub>y</sub>	-0.0341	0.0
		2p <sub>z</sub>	0.0283	0.0
$E_x = 0.1$	H <sub>1</sub>	1s	-0.0101	0.0150
		1s	0.0000990	0.0
	C <sub>1</sub>	2s	0.0449	0.0
		2p <sub>x</sub>	-0.0026	0.0
		2p <sub>y</sub>	0.0087	0.0
		2p <sub>z</sub>	0.0431	0.0
	C <sub>2</sub>	1s	0.0000402	0.0
		2s	0.0030	0.0
		2p <sub>x</sub>	0.0153	0.0
		2p <sub>y</sub>	0.0639	0.0
$E_z = 0.1$		2p <sub>z</sub>	-0.0125	0.0
		H <sub>1</sub>	0.0179	-0.0099
	H <sub>3</sub>	1s	0.0386	-0.0195
		1s	0.0000265	0.0000827
	C <sub>1</sub>	2s	0.0227	0.0185
		2p <sub>x</sub>	-0.0078	0.0156
		2p <sub>y</sub>	-0.0344	0.0179
		2p <sub>z</sub>	0.0288	0.0058
	H <sub>1</sub>	1s	-0.0103	0.0102
		H <sub>2</sub>	-0.0096	0.0401

<sup>a</sup> See Figure 2 for orientations and numbering of atoms.

electric fields can be realized experimentally in the future. Moreover, it would also give a guiding idea in analyzing the effects of *local* electric fields which appear more frequently in chemistry. To establish the general utility of the model, it is necessary to test it with a larger number of molecules of different types. In a

subsequent paper, we will show the results of such examinations.

**Acknowledgment.** We started this study stimulated by the lectures of and discussions with Professor Zahradnik, who visited our department in December 1977. One of the authors (H.N.) would like to gratefully acknowledge Professor Zahradnik for this and stimulating discussion. We also want to thank Mrs. S. Kanayama and K. Kanda for valuable assistances in programming. This study was supported in part by a Grant-in-Aid for Scientific Research from the Japanese Ministry of Education, Science and Culture.

#### Appendix A. Effect of Floating

Table VI shows the energy lowering due to the floating. It is very large for CO. As expected, the effect of floating is larger in the electric field than in the absence of the field, except for NH<sub>3</sub> ( $E_z = -0.1$  au) and CO ( $E_x = 0.1$  au). The difference is large especially for CH<sub>4</sub> since in the absence of the field the AOs on carbon do not float away from the nucleus because of the  $T_d$  symmetry. In Table VII we show the optimal centers of the floating AOs for ethylene in the field  $E_x = 0.1$  au. When the electric field is applied, the AOs move in the direction of the field. The most sensitive AOs are the 1s AOs of hydrogens, and the next are the 2s and 2p AOs of carbon.

#### Appendix B

We consider the symmetry properties of the reorganized density  $\Delta\rho$  induced by the electric field. We take ethylene with  $E_x = 0.1$  au as an example but the result is very general. The origin is taken at the center of the C-C bond. Let  $\psi_0$  be the ground-state wave function in the absence of the field. Under the field the wave function may be written as

$$\psi = \psi_0 + \psi'$$

$$\psi' = \sum_n \frac{\langle \psi_n | H' | \psi_0 \rangle}{E_n - E_0} \psi_n \quad (\text{B1})$$

to first order in the perturbation  $H' = E \cdot x$ . Since  $\psi_0$  is symmetric i.e.,  $\psi_0(-x) = \psi_0(x)$ ,  $\psi'$  should be antisymmetric,  $\psi'(-x) = -\psi'(x)$ , in order that the numerator in eq B1 be nonzero. The electron density is calculated as

$$\rho = N\{\langle \psi_0 | \psi_0 \rangle_1 + 2\langle \psi_0 | \psi' \rangle_1 + \langle \psi' | \psi' \rangle_1\} \quad (\text{B2})$$

where  $\langle \rangle_1$  denotes integration over the coordinates of all the  $N$  electrons except for the first one. Neglecting the last term we obtain

$$\Delta\rho = 2N\langle \psi_0 | \psi' \rangle_1 \quad (\text{B3})$$

From the symmetry property of the  $\psi_0$  and  $\psi'$ , we get

$$\Delta\rho(-x) = -\Delta\rho(x) \quad (\text{B4})$$

Thus, the reorganized density  $\Delta\rho$  is almost antisymmetric with respect to the origin. Note that the last term of eq B2 is symmetric.